Atmos. Chem. Phys. Discuss., doi:10.5194/acp-2016-1110, 2016
Manuscript under review for journal Atmos. Chem. Phys.
Published: 20 December 2016

Atmospheric Chemistry and Physics Discussions

Sixty years of radiocarbon dioxide measurements at Wellington, New Zealand 1954 – 2014

Jocelyn C. Turnbull[1,2,*] Sara E. Mikaloff Fletcher[3], India Ansell[1], Gordon Brailsford[3], Rowena Moss[3], Margaret Norris[1], Kay Steinkamp[3]

[1]GNS Science, Rafter Radiocarbon Laboratory, Lower Hutt, New Zealand
[2]CIRES, University of Colorado at Boulder, Boulder, Colorado, USA
[3]NIWA, Wellington, New Zealand
* contact author: j.turnbull@gns.cri.nz

1. Abstract

We present 60 years of $\Delta^{14}CO_2$ measurements from Wellington, New Zealand (41°S, 175°E). The record has been extended and fully revised. New measurements have been used to evaluate the existing record and to replace original measurements where warranted. This is the earliest atmospheric $\Delta^{14}CO_2$ record and records the rise of the ^{14}C "bomb spike", the subsequent decline in $\Delta^{14}CO_2$ as bomb ^{14}C moved throughout the carbon cycle and increasing fossil fuel CO_2 emissions further decreased atmospheric $\Delta^{14}CO_2$. The initially large seasonal cycle in the 1960s reduces in amplitude and eventually reverses in phase, resulting in a small seasonal cycle of about 2 ‰ in the 2000s. The seasonal cycle at Wellington is dominated by the seasonality of cross-tropopause transport, and differs slightly from that at Cape Grim, Australia, which is influenced by anthropogenic sources in winter. $\Delta^{14}CO_2$ at Cape Grim and Wellington show very similar trends, with significant differences only during periods of known measurement uncertainty. In contrast, Northern Hemisphere clean air sites show a higher and earlier bomb ^{14}C peak, consistent with a 1.4-year interhemispheric exchange time. From the 1970s until the early 2000s, the Northern and Southern Hemisphere $\Delta^{14}CO_2$ were quite similar, apparently due to the balance of ^{14}C-free fossil fuel CO_2 emissions in the north and ^{14}C-depleted ocean upwelling in the south. The Southern Hemisphere sites show a consistent and marked elevation above the Northern Hemisphere sites since the early 2000s, which is most likely due to reduced upwelling of ^{14}C-depleted and carbon-rich deep waters in the Southern Ocean. This developing $\Delta^{14}CO_2$ interhemispheric gradient is consistent with recent studies that indicate a reinvigorated Southern Ocean carbon sink since the mid-2000s, and suggests that upwelling of deep waters plays an important role in this change.

Atmos. Chem. Phys. Discuss., doi:10.5194/acp-2016-1110, 2016
Manuscript under review for journal Atmos. Chem. Phys.
Published: 20 December 2016

Atmospheric Chemistry and Physics Discussions

2. Introduction

Measurements of radiocarbon in atmospheric carbon dioxide ($\Delta^{14}CO_2$) have long been used as a key to understanding the global carbon cycle. The first atmospheric $\Delta^{14}CO_2$ measurements were begun at Wellington, New Zealand in 1954 (Rafter, 1955; Rafter et al., 1959), aiming to better understand carbon exchange processes (Otago Daily Times, 1957). Northern Hemisphere $\Delta^{14}CO_2$ measurements began a few years later in Norway (Nydal and Løvseth, 1983) and Austria (Levin et al., 1985).

^{14}C is a cosmogenic nuclide produced naturally in the upper atmosphere through neutron spallation, exchanges to form $^{14}CO_2$ and then moves throughout the global carbon cycle. Production is roughly balanced by radioactive decay, which mostly occurs in the carbon-rich and slowly overturning ocean carbon reservoir and to a lesser extent in the faster cycling terrestrial carbon reservoir. The perturbations to $\Delta^{14}CO_2$ from atmospheric nuclear weapons testing in the mid-20th century and additions of ^{14}C-free CO_2 from fossil fuel burning have both provided tools to investigate CO_2 sources and sinks.

Penetration of bomb-^{14}C into the oceans has been used to understand ocean carbon uptake processes (Oeschger et al., 1975; Broecker et al., 1985; Key et al., 2004; Sweeney et al., 2007; Naegler et al., 2006). Terrestrial biosphere carbon residence times and exchange processes have also been widely investigated using bomb-^{14}C (e.g. Trumbore et al., 2000; Naegler et al., 2009). Stratospheric residence times, cross-tropopause transport and interhemispheric exchange can also be examined with atmospheric $\Delta^{14}CO_2$ observations (Kanu et al., 2015; Kjellström et al., 2000).

The Suess Effect, the decrease in atmospheric $\Delta^{14}CO_2$ due to the addition of ^{14}C-free fossil fuel CO_2, was first identified in 1955 (Suess, 1955). It has subsequently been refined (Levin et al., 2003; Turnbull et al., 2006) and used to investigate fossil fuel CO_2 additions at various scales (e.g. Miller et al., 2012; Turnbull et al., 2009; Lopez et al., Turnbull et al., 2015; Djuricin et al., 2010).

The full atmospheric ^{14}C budget has been investigated using long term $\Delta^{14}CO_2$ records in conjunction with atmospheric transport models (Randerson et al., 2002; Caldiera et al., 1998; Levin et al., 2010; Turnbull et al., 2009; Naegler et al., 2006). These have shown changing controls on $\Delta^{14}CO_2$ through time. Prior to nuclear weapons testing, natural cosmogenic production added ^{14}C in the upper atmosphere, which reacted to CO_2 and moved throughout the atmosphere and the carbon cycle. The short carbon residence time in the biosphere meant that biospheric exchange processes had only a small influence on $\Delta^{14}CO_2$, whereas the ocean exerted a stronger influence due to radioactive decay during its much longer (and temporally varying) turnover time. The addition of bomb ^{14}C in the 1950s and 1960s almost doubled the atmospheric ^{14}C content. This meant that both the ocean and biosphere were now very ^{14}C-poor relative to the atmosphere. As the bomb-^{14}C was distributed throughout the carbon cycle, this impact weakened, and by the 1990s, the additions of fossil fuel CO_2 became dominant.

The long-term $\Delta^{14}CO_2$ records have been crucial in all of these findings, and the Wellington $\Delta^{14}CO_2$ record is of especial importance, being the oldest direct atmospheric

Atmos. Chem. Phys. Discuss., doi:10.5194/acp-2016-1110, 2016
Manuscript under review for journal Atmos. Chem. Phys.
Published: 20 December 2016

trace gas record, even predating the CO_2 mole fraction record started at Mauna Loa in 1958 (Keeling, 1961; Keeling and Whorf, 2005). It is the only Southern Hemisphere record recording the bomb spike. Several short Southern Hemisphere records do exist (Meijer et al., 2006; Graven et al., 2012b; Manning et al., 1990; Hua and Barbetti 2013), and some longer records began in the 1980s (Levin et al., 2010). Over the more than 60 years of measurement, there have necessarily been changes in how the Wellington samples are collected and measured. There are no comparable records during the first 30 years of measurement, so that the data quality has not been independently evaluated. Comparison with other records since the mid-1980s has suggested that there may be biases in some parts of the Wellington record (Currie et al., 2011).

Here we present a revised and extended Wellington atmospheric $^{14}CO_2$ record, spanning 60 years from December 1954 to December 2014. We detail the different sampling, preparation and measurement techniques used through the record, compare with new tree ring measurements, discuss revisions to the previously published data and provide a final dataset with accompanying smooth curve fit.

In the results and discussion, we revisit the key findings that the Wellington $^{14}CO_2$ record has provided over the years and expand with new findings based on the most recent part of the record. The most recent publication of this dataset included data to 2005 (Currie et al., 2011) and showed periods of variability and a seasonal cycle at Wellington that differ markedly from the independent Cape Grim, Tasmania $^{14}CO_2$ record at a similar southern latitude (Levin et al., 2010). Here we add complementary new data to investigate these differences, fill gaps and extend the record to near-present. We examine an emerging interhemispheric gradient in $^{14}CO_2$, which supports evidence of a changing Southern Ocean carbon sink. If this emerging gradient is indeed linked to Southern Ocean processes, it suggests that ocean circulation plays a substantive role in the reinvigoration of the Southern Ocean carbon sink.

3. Methods

Over 60 years of measurement, a number of different sample collection, preparation, measurement and reporting methods have been used. In this section, we give an overview of the various methods and changes through time, and they are summarized in table 1. Full details of the sampling methods used through time are provided in the supplementary material, compiling methodological information documented in previous reports on the Wellington record (Rafter and Fergusson, 1959; Manning et al., 1990; Currie et al., 2011) along with methods newly applied in this new extension and refinement of the dataset.

3.1. Sampling sites

Samples from 15 December 1954 – 5 June 1987 were collected at Makara (Lowe, 1974), on the south-west coast of the North Island of New Zealand (MAK, 41.25°S, 174.69°E, 300 m asl). Samples since 8 July 1988 have been collected at Baring Head (Brailsford et al., 2012) on the South Coast of the lower North Island and 23 km southeast of Makara (BHD, 41.41°S, 174.87°E, 80 m asl) (figure 1). We also discuss tree ring samples collected from Eastbourne, 12 km north of Baring Head on Wellington Harbour.

Atmos. Chem. Phys. Discuss., doi:10.5194/acp-2016-1110, 2016
Manuscript under review for journal Atmos. Chem. Phys.
Published: 20 December 2016

Atmospheric Chemistry and Physics Discussions

3.2. Collection methods

3.2.1. NaOH absorption

The primary collection method is static absorption of CO_2 into nominally CO_2-free 0.5 or 1 M L^{-1} sodium hydroxide (NaOH) solution, which is left exposed to air at the sampling site providing an integrated sample over a period of ~2 weeks (Rafter, 1955). From 1954-1995, ~ 2 L NaOH solution was exposed to air in a large Pyrex® tray. Since 1995, high-density polyethylene (HDPE) bottles containing ~200 mL NaOH solution were left open inside a Stevenson meteorological screen; the depth of the solution in the bottles remained the same as that in the previously used trays. No significant difference has been observed between the two methods (Currie et al., 2011). A few early (1954-1970) samples were collected using different vessels, air pumped through the NaOH (vs. passive absorption), or NaOH was replaced with barium hydroxide (Rafter, 1955; Manning et al., 1990). CO_2 is extracted from the NaOH solution by acidification followed by cryogenic distillation (Rafter and Fergusson, 1959; Currie et al., 2011).

3.2.2. Whole air flasks

In this study, we use whole air flask samples collected at Baring Head to supplement and/or replace NaOH samples. Flasks of whole air are collected by flushing ambient air through the flask for several minutes then filled to slightly over ambient pressure. Most flasks were collected during southerly, clean air conditions (Stephens et al., 2013). CO_2 is extracted cryogenically (Turnbull et al., 2015). For whole air samples collected from 1984-1993, the extracted CO_2 was archived until 2012. We evaluated the quality of this archived CO_2 using two methods. Tubes with major leakage were readily detected by air present in the tube and were discarded. $\delta^{13}C$ from all the remaining samples was in agreement with $\delta^{13}C$ measured from separate flasks collected at Baring Head and measured for $\delta^{13}C$ by Scripps Institution of Oceanography at close to the time of collection (http://scrippsco2.ucsd.edu/data/nzd). Whole air samples collected since 2013 are analyzed for $\delta^{13}C$ and other trace gases and isotopes at NIWA (Ferretti et al., 2000) and for the $^{14}CO_2$ measurement, CO_2 is extracted from whole air at Rafter Radiocarbon Laboratory (Turnbull et al., 2015).

3.2.3. Tree rings

When trees photosynthesize, they faithfully record the ^{14}C content of ambient CO_2 in their cellulose, the structural component of wood. Annual tree rings therefore provide a summertime (approximately September – April in the Southern Hemisphere) daytime average $\Delta^{14}CO_2$. Photosynthetic uptake varies during the daylight hours depending on factors including growth period, sunlight, and temperature (Bozhinova et al., 2013), resulting in a somewhat different effective sampling pattern than the 1-2 week NaOH solution collections. We show in section 3.5.1. that at the Wellington location this difference is negligible. Note that we assign the mean age of each ring as January 1 of the year in which growth finished (i.e. the mean age of a ring growing from September – April), whereas dendrochronologists assign the "ring year" is as the year in which ring growth started (i.e. the previous year).

We collected cores from three trees close to the Baring Head site. A pine (*Pinus radiata*) located 10 m from the Baring Head sampling station (figure 1) yielded rings back to 1986

Atmos. Chem. Phys. Discuss., doi:10.5194/acp-2016-1110, 2016
Manuscript under review for journal Atmos. Chem. Phys.
Published: 20 December 2016

Atmospheric Chemistry and Physics Discussions

(Norris, 2015). A longer record was obtained from two New Zealand kauri (*Agathis australis*) specimens planted in 1919 and 1920, located 20 m from one another in Eastbourne, 12 km from Baring Head (figure 1). Kauri is a long-lived hardwood species that has been widely used in dendrochronology and radiocarbon calibration studies (e.g. Hogg et al., 2013).

Annual rings were counted from each core. Shifting the Eastbourne record by one year in either direction moves the ^{14}C bomb spike maximum out of phase with the NaOH-based Wellington $\Delta^{14}CO_2$ record (supplementary figure S1), confirming that the ring counts are correct. For the Baring Head pine, rings go back to only 1986, and we verify them by comparing with the Eastbourne record. They show an insignificant mean difference of -0.4 ± 0.8 ‰ (supplementary figure S1).

In practice, it is difficult to ensure that one annual ring is sampled without losing any material from that ring, and no wood from surrounding rings is included. To evaluate the potential bias from this source, we measured replicate samples from different cores from the same tree (Baring Head) or two different trees (Eastbourne, 12 km north of Baring Head). For samples collected since 1985, all these replicates agree within one standard deviation (supplementary figure S2). However, for three replicates from Eastbourne in 1963, 1965 and 1971, we see large differences of 9.2, 44.5 and 4.9 ‰, which we attribute to small differences in sampling of the rings that were magnified by the rapid change in $\Delta^{14}C$ of up to 200 ‰ yr^{-1} during this period. Thus, the tree ring $\Delta^{14}C$ values during this period should be treated with caution.

Cellulose was isolated from whole tree rings by first removing labile organics with solvent washes, then oxidation to isolate the cellulose from other materials (Norris, 2015; Hua et al., 2000). The cellulose was combusted and the CO_2 purified following standard methods in the Rafter Radiocarbon Laboratory (Baisden et al., 2013).

3.3. ^{14}C measurement

Static NaOH samples were measured by conventional decay counting on the CO_2 gas from 1954 – 1995 (Manning et al., 1990; Currie et al., 2011) and these are identified by their unique "NZ" numbers. All measurements made since 1995, including recent measurements of flask samples collected in the 1980s and 1990s, were reduced to graphite, measured by accelerator mass spectrometry (AMS), and are identified by their unique "NZA" numbers. The LG1 graphitization system was used from 1995 to 2011 (NZA < 50,000) (Lowe et al., 1987), and replaced with the RG20 graphite system in 2011 (NZA > 50,000) (Turnbull et al., 2015). Samples measured by AMS were stored for up to three years between sample collection and extraction/graphitization/measurement.

For samples collected from 1995 to 2010, an EN Tandem AMS was used for measurement (NZA < 35,000, Zondervan and Sparks, 1996). Until 2005 (NZA <30,000, including all previously reported Wellington $^{14}CO_2$ data), only ^{13}C and ^{14}C were measured on the EN Tandem system, so the normalization correction for isotopic fractionation (Stuiver and Polach, 1977) was performed using an offline isotope ratio mass spectrometer $\delta^{13}C$ value. The data reported from 2005 onwards (NZA > 30,000)

Atmos. Chem. Phys. Discuss., doi:10.5194/acp-2016-1110, 2016
Manuscript under review for journal Atmos. Chem. Phys.
Published: 20 December 2016

Atmospheric Chemistry and Physics Discussions

show a reduction in scatter reflecting the addition of online ^{12}C measurement in the EN Tandem system in 2005. This allows direct online correction for isotopic fractionation that may occur during sample preparation and in the accelerator itself (Zondervan et al., 2015), and results in improved long-term repeatability.

For all EN Tandem samples, a single large aliquot of extracted CO_2 was split into four separately graphitized and measured targets and the results of all four were averaged. We have revisited the multi-target averaging, applying a consistent criterion to exclude outliers and using a weighted mean of the retained measurements (supplementary material). This results in differences of up to 5 ‰ relative to the values reported by Currie et al. (2011).

In 2010, the EN Tandem was replaced with a National Electrostatics Corporation AMS, dubbed XCAMS (NZA > 34,000). XCAMS measures all three carbon isotopes, such that the normalization correction is performed using the AMS measured ^{13}C values (Zondervan et al., 2015). XCAMS measurements are made on single graphite targets measured to high precision (Turnbull et al., 2015).

3.4. Results format

NaOH samples are collected over a period of typically two weeks, and sometimes much longer. We report the date of collection as the average of the start and end dates. In cases where the end date was not recorded, we use the start date. For a few samples, the sampling dates were not recorded or are ambiguous, and those results have been excluded from the reported dataset.

Results are reported here as $F^{14}C$ (Reimer et al., 2004) and $\Delta^{14}C$ (Stuiver and Polach, 1977). $F^{14}C$ is corrected for isotopic fractionation and blank corrected. We calculated $F^{14}C$ from the original measurement data recorded in our databases, and updated a handful of records where transcription errors were found. $\Delta^{14}C$ is derived from $F^{14}C$, and corrected for radioactive decay since the time of collection (Stuiver and Polach, 1977). $\Delta^{14}C$ has been recalculated using the date of collection for all results, resulting in changes of a few tenths of permil in most $\Delta^{14}C$ values relative to those reported by Currie et al. (2011) and Manning et al. (1990). Uncertainties are reported based on the counting statistical uncertainty and for AMS measurements we add an additional error term, determined from the long-term repeatability of secondary standard materials (Turnbull et al., 2015). Samples for which changes have been made relative to the previously published results are indicated by the quality flag provided in the supplementary dataset. Where more than one measurement was made for a given date, we report the weighted mean of all measurements.

3.5. Data validation

3.5.1. Tree ring comparison

Over the more than 60 years of the Wellington $\Delta^{14}CO_2$ record, there have necessarily been many changes in methodology, and the tree rings provide a way to validate the full record, albeit with lower resolution. Due to the possible sampling biases in the tree rings

Atmos. Chem. Phys. Discuss., doi:10.5194/acp-2016-1110, 2016
Manuscript under review for journal Atmos. Chem. Phys.
Published: 20 December 2016

Atmospheric Chemistry and Physics Discussions

(section 3.2.3.), we do not include them in the final updated record, but use them to validate the existing measurements.

During the rapid $\Delta^{14}CO_2$ change in the early 1960s, there are some differences between the kauri tree ring and Wellington $\Delta^{14}CO_2$ records. The 1963 and 1964 tree ring samples are slightly lower than the concurrent $\Delta^{14}CO_2$ samples. The peak $\Delta^{14}CO_2$ measurement in the tree rings is 30 ‰ lower than the smoothed $\Delta^{14}CO_2$ record, and 100‰ lower than the two highest $\Delta^{14}CO_2$ measurements in 1965. These differences are likely due to small errors in sampling of the rings, which will be most apparent during periods of rapid change.

Prior to 1960 and from the peak of the bomb spike in 1965 until 1990, there is remarkable agreement between the tree rings and Wellington $\Delta^{14}CO_2$ record, with the wiggles in the record replicated in both records. And since 2005, there is excellent agreement across all the different records. Some differences are observed in 1990-1993 and 1995-2005, which we discuss in the following sections.

3.5.2. 1990-1993 excursion

An excursion in the gas counting measurements between 1990 and 1993 has previously been noted (figures 2, 3) as a deviation from the Cape Grim $\Delta^{14}CO_2$ record (Levin et al., 2010) during the same period. Cape Grim is at similar latitude, and observes a mixture of air from the mid-latitude Southern Ocean sector and terrestrial Australia (Law et al., 2010; Ziehn et al., 2014). The Wellington and Cape Grim records overlap during almost all other periods (figure 3).

We use archived CO_2 from flask samples to evaluate this period of deviation. First, the recent flask samples collected since 2013 (n=12) agree very well with the NaOH static samples from the same period (figure 2), indicating that despite the difference in sampling period for the two methods, flask samples reflect the $\Delta^{14}CO_2$ observed in the longer-term NaOH static samples. We then selected a subset of archived 1984 - 1992 extracted CO_2 samples for measurement, mostly from Southerly wind conditions, but including a few from other wind conditions. These flask $\Delta^{14}CO_2$ measurements do not exhibit the excursion seen in the NaOH static samples (figure 2), implying that the deviation observed in the original NaOH static samples may be a consequence of sampling, storage or measurement errors. Annual tree rings from both the kauri and pine follow the flask measurements for this period (figure 2), confirming that the NaOH static samples are anomalous.

The 1990-1993 period was characterized by major changes in New Zealand science, both in the organizational structure and personnel. Although we are unable to exactly reconstruct events at that time, we hypothesize that the NaOH solution preparation was conducted slightly differently, perhaps omitting the barium chloride precipitation step for these samples. This would result in contaminating CO_2 absorbed on the NaOH before the solution was prepared, which would result in higher $\Delta^{14}CO_2$ observed in these samples than in the ambient air. In any case, these values are anomalous and we remove the

Atmos. Chem. Phys. Discuss., doi:10.5194/acp-2016-1110, 2016
Manuscript under review for journal Atmos. Chem. Phys.
Published: 20 December 2016

original NaOH static sample measurements between 1990 and 1993 and replace them with the new flask measurements for the same period.

3.5.3. 1995-2005 variability

As already discussed in section 3.3, the measurement method was changed from gas counting to AMS for samples collected in 1995 or thereafter. During the first ten years of AMS measurements, the record is much noisier than during any other period (figure 2). In 2005, online ^{12}C measurement was added to the AMS system, substantially improving the measurement accuracy (Zondervan et al., 2015), and the noise in the $\Delta^{14}CO_2$ record immediately reduced.

The remaining NaOH solution for all samples collected since 1995 has been archived, and typically only every second sample collected was measured, with the remainder archived without sampling. In 2011-2016, we revisited the 1995-2005 period, remeasuring some samples that had previously been measured and some that had never been measured for a total of 52 new analyses.

The new measurements on this period do show reduced scatter over the original analyses, particularly for the period from 1998-2001 where the original analyses appear anomalously low and in 2002-2003 when the original analyses appear anomalously high. Yet there remain a number of both low and high outliers in the new measurements. These are present in both the samples that were remeasured and in those for which this was the first sample from the bottle. This suggests that a subset of the archived sample bottles were either contaminated at the time of collection, or that some bottles were insufficiently sealed, causing contamination with more recent CO_2 during storage. Comparison with the tree ring measurements and with the Cape Grim record (Levin et al., 2010) suggest that the measurements during this period may, on average, be biased high as well as having additional scatter (figure 3). Nonetheless, in the absence of better data, we retain both the original and remeasured NaOH sample results in the full record.

3.6. Smooth curve fit

In addition to the raw measured $\Delta^{14}CO_2$ values, we calculate a smooth curve fit and deseasonalized trend from the Wellington $\Delta^{14}C$ and $F^{14}C$ datasets. The deseasonalized trend may be more useful than the raw data for aging of recent materials (e.g. Reimer et al., 2004; Hua et al., 2013). Acknowledging that the 1995-2005 period is variable and possibly biased in the Wellington record, we also provide in the supplementary material an alternative mid-latitude Southern Hemisphere smooth curve fit and deseasonalized trend in which the Wellington data for 1995-2005 has been removed and replaced with the Cape Grim data for that period (Levin et al., 2010).

Curvefitting is particularly challenging for the $\Delta^{14}CO_2$ record, since (a) there are data gaps and inconsistent sampling frequency, (b) the growth rate and trend vary dramatically and (c) the seasonal cycle changes both in magnitude and phase (section 4.2). We chose to use the ccgvu fitting procedure (Thoning et al., 1989), which uses fast Fourier transform and low-pass filtering techniques to obtain a smoothed seasonal cycle and long term trend from atmospheric data. This technique can readily handle the data gaps and

Atmos. Chem. Phys. Discuss., doi:10.5194/acp-2016-1110, 2016
Manuscript under review for journal Atmos. Chem. Phys.
Published: 20 December 2016

Atmospheric Chemistry and Physics Discussions

inconsistent sampling frequency in our record, whereas the other widely used fitting procedure, seasonal trend decomposition using locally weighted scatter plot smoothing (STL) requires gap-filling for our dataset (e.g. Pickers et al., 2015). However, ccgvu assigns a single set of harmonic terms across the full time period, which is inappropriate in this case of large variation in the seasonal cycle. Thus, we separate the record into five time periods, chosen as periods when changes in the growth rate, seasonal cycle and data quality change: 1954-1965, 1966-1979, 1980-1989, 1990-2004, 2005-2014. For each time period, we use ccgvu with one linear and two harmonic terms and fit residuals are added back using a low-pass filter with an 80 cutoff in the frequency domain. At each transition, we overlapped a two-year period and linearly interpolated the two fits across that two year period to smooth the transitions caused by end effects. The deseasonalized trend was determined from the full dataset rather than the five time periods, as it does not include the seasonality and produces the same result in either case.

The mean residual difference between the fitted curve and the measured $\Delta^{14}CO_2$ values is 3.8 ‰, consistent with the typical measurement uncertainty for the full dataset. Further, the residuals are highest for the early period (1954-1970) at 6 ‰, consistent with the larger measurement errors at that time of ~6 ‰. The residuals improve as the measurement errors reduce, such that since 2005, the mean residual is 2 ‰, consistent with the reported 2 ‰ uncertainties. The exception is the 1995- 2005 period where the mean residual difference of 5 ‰ is substantially higher than the mean reported uncertainty of 2.5 ‰, reflecting the apparent larger scatter during this period as discussed in section 3.5.3.

The one-sigma uncertainty on the smoothed curve and deseasonalized trend were determined using a Monte Carlo technique. Each data point was perturbed by a random normal error based on the reported uncertainty of that data point, such that the standard deviation of all perturbations would equal the reported uncertainty to derive the one-sigma and 95% confidence interval for the smooth curve.

3.7 Atmospheric Model Simulations

Simulations from the Numerical Atmospheric dispersion Modelling Environment (NAME) III Lagrangian dispersion model (Jones et al., 2007) were used to interpret seasonal variability in the dataset. The NAME model is run backwards in time to analyse the history of the air traveling towards BHD and LAU over the preceding 4 days. For each day of the simulation period, 10,000 particles were released during two time windows in the afternoon; 13:00-14:00 and 15:00-16:00. NAME was driven by meteorological output from the New Zealand Limited Area Model-12 (NZLAM-12), a local configuration of the UK Met Office Unified Model (Davies et al., 2007.) NZLAM has a horizontal resolution of ~12 km, with 70 vertical levels ranging from the earth's surface to 80km. These simulations have been described in more detail by Steinkamp et al. (2016). The average footprints presented here were computed by summing the footprints for every day and release period in 2011-2013 and normalizing them such that the domain integral equals one.

Atmos. Chem. Phys. Discuss., doi:10.5194/acp-2016-1110, 2016
Manuscript under review for journal Atmos. Chem. Phys.
Published: 20 December 2016

Atmospheric Chemistry and Physics Discussions

4. Results and Discussion

4.1. Variability in the Wellington record through time

The Wellington $\Delta^{14}CO_2$ record begins in December 1954, at a roughly "natural" pre-bomb $\Delta^{14}CO_2$ level of -20 ‰. From 1955, $\Delta^{14}CO_2$ increased rapidly, near doubling to 700 ‰ in 1965 at Wellington, due to the production of ^{14}C during atmospheric nuclear weapons tests. Nuclear tests in the early 1950s contributed to the rise, then a hiatus in testing in the late 1950s led to a plateau in Wellington $\Delta^{14}CO_2$ before a series of very large atmospheric tests in the early 1960s led to further increases (Rafter and Ferguson, 1959; Manning et al., 1990).

Most atmospheric nuclear weapons testing ceased in 1963, and the Wellington $\Delta^{14}CO_2$ record peaks in 1965 then begins to decline, at first rapidly at -30 ‰ yr^{-1} in the 1970s and gradually slowing to -5 ‰ yr^{-1} since 2005. The initial rapid decline has been attributed primarily to the uptake of the excess radiocarbon into the oceans, and to a lesser extent, uptake into the terrestrial biosphere (Stuiver and Quay 1981; Manning et al., 1990; Naegler et al 2006; Randerson et al., 2002). The short residence time of carbon in the biosphere means that from the 1980s, the terrestrial biosphere changed from a ^{14}C sink to a ^{14}C source as the bomb pulse was re-released (Randerson et al., 2002; Levin et al., 2010; Turnbull et al., 2009).

Natural cosmogenic production of ^{14}C damps the long-term decline, increasing $\Delta^{14}CO_2$ by 5 ‰ yr^{-1}; this may vary with the solar cycle, but there is no long-term trend in this component of the signal (Turnbull et al., 2009; Naegler et al., 2006). There is also a small positive contribution from the nuclear industry which emits ^{14}C to the atmosphere, and this has increased from zero in the 1950s to 0.5 – 1 ‰ yr^{-1} in the last decade (Graven and Gruber, 2011; Turnbull et al., 2009; Levin et al., 2010).

The Suess Effect, the decrease in atmospheric $\Delta^{14}CO_2$ due to the addition of ^{14}C-free fossil fuel CO_2 to the atmosphere (Suess 1955; Tans 1979; Levin et al., 2003), was first recognized in 1955 and has played a role throughout the record. Although the magnitude of fossil fuel CO_2 emissions has grown through time, when convolved with the declining atmospheric $\Delta^{14}CO_2$ history, the impact on $\Delta^{14}CO_2$ has stayed roughly constant at -10 ‰ yr^{-1} since the 1970s (Levin et al., 2010; Randerson et al., 2002). Since the 1990s, the Suess Effect has been the dominant driver of the ongoing negative growth rate (Levin et al., 2010; Turnbull et al., 2009).

4.2. Seasonal variability in the Wellington record

We determine the changing seasonal cycle from smooth curve fits to five separate periods of the record (1954-1965, 1966-1979, 1980-1989, 1990-2004, 2005-2014). This subdivision is necessary to allow the seasonal cycle to vary through time since the ccgvu curve fitting routine assigns a single set of harmonics to the time period fitted (see section 3.6). The 1966-1979 period shows a strong seasonal cycle (figure 4) of about 30‰ amplitude, which is primarily attributed to seasonally varying stratosphere – troposphere exchange bringing bomb ^{14}C into the troposphere (Manning et al., 1990; Randerson et al.,

Atmos. Chem. Phys. Discuss., doi:10.5194/acp-2016-1110, 2016
Manuscript under review for journal Atmos. Chem. Phys.
Published: 20 December 2016

Atmospheric Chemistry and Physics Discussions

2002). Manning et al. (1990) were unable to simulate the correct phasing of the seasonal cycle, apparently because their model distributed bomb ^{14}C production throughout both Northern and Southern stratosphere. In fact, the majority of the bomb ^{14}C was produced in the Northern Hemisphere stratosphere (Enting et al., 1982), and we show schematically in figure 5 why this causes the opposite seasonal phase. Most transport across the equator occurs in the troposphere, so that the Southern Hemisphere stratosphere would have had a lower $\Delta^{14}CO_2$ than the Southern Hemisphere troposphere during the early post-bomb period (figure 6). Since maximum cross-tropopause exchange occurs in the spring (Olsen et al., 2003), this resulted in a minimum in $\Delta^{14}CO_2$ at Wellington in the austral spring (August) when bomb ^{14}C moved most rapidly into the stratosphere. The seasonal cycle kept the same phase but gradually decreased in amplitude until the late 1970s, attributed to the declining disequilibrium between the stratosphere and troposphere as the bomb ^{14}C moved throughout the carbon reservoirs.

Between 1978 and 1980 the seasonal cycle weakened, and then reversed during the 1980s, with a maximum in winter (June – August) and amplitude of about 5 ‰. This result is comparable to that obtained by Manning et al. (1990) and Currie et al. (2011), who both used a seasonal trend loess (STL) procedure to determine the seasonal cycle from the same data. We hypothesize that as tropospheric $\Delta^{14}CO_2$ declined, and continued natural production of ^{14}C occurred in the stratosphere, the Southern Hemisphere stratosphere eventually became enriched in ^{14}C relative to the Southern Hemisphere troposphere, so that consistent seasonally varying exchange processes resulted in a change in sign of cross-tropopause $\Delta^{14}CO_2$ exchange in the late 1970s (figure 5). To the best of our knowledge, no Southern Hemisphere stratosphere $\Delta^{14}CO_2$ measurements have been made since the mid-1970s, so there is no direct evidence for this hypothesis.

The Wellington $\Delta^{14}CO_2$ seasonal cycle declined in the 1990s, and the larger variability in the observations between 1995 and 2005 makes it difficult to discern a seasonal cycle during that period. Since 2005, the more precise measurements allow us to detect a small seasonal cycle with amplitude of about 2 ‰ (figure 4). Measurements from Cape Grim, Australia from 1995-2010 show a similar magnitude seasonal cycle to that at Wellington from 2005 - 2015, and a maximum in March – April that coincides with a seasonal maximum in the Wellington record (Levin et al., 2010). However, Wellington $\Delta^{14}CO_2$ exhibits a second maximum in the austral spring (October) that is not apparent at Cape Grim. Recent work has shown that during the winter, the Cape Grim station is influenced by air coming off the Australian mainland including the city of Melbourne (Ziehn et al., 2014), which would act to reduce $\Delta^{14}CO_2$ at Cape Grim relative to Southern Ocean clean air. In contrast, the Baring Head location near Wellington is not significantly influenced by urban regions in any season (figure 6). Air is typically from the ocean, and the local geography means that the urban emission plume from Wellington and its northern suburbs of Lower Hutt very rarely passes over Baring Head, and the typically high wind speeds further reduce the influence of the local urban area (Stephens et al., 2013). During the austral autumn, there is some land influence from the Christchurch region in the South Island, but emissions from Christchurch are much smaller than the Melbourne emissions influencing Cape Grim (State of Victoria fossil fuel CO_2 emissions for 2013 were 23 MtC, Wellington and Christchurch each emitted 0.4

Atmos. Chem. Phys. Discuss., doi:10.5194/acp-2016-1110, 2016
Manuscript under review for journal Atmos. Chem. Phys.
Published: 20 December 2016

Atmospheric Chemistry and Physics Discussions

MtC of fossil fuel CO_2 in 2012/13 (AECOM, 2016; Australian Government, 2016; Boden et al., 2012)). The observed Baring Head $\Delta^{14}CO_2$ maximum in spring in the recent part of the record can be explained by the seasonal maximum in cross-tropopause exchange bringing ^{14}C-enriched air at this time of year (figure 5).

4.3. Comparison with other atmospheric $\Delta^{14}CO_2$ records

We compare the Wellington $\Delta^{14}CO_2$ record with several other $\Delta^{14}CO_2$ records that are indicated in figure 1. First, we compare with measurements from Cape Grim, Australia (CGO, 40.68°S, 144.68°E, 94 m asl). Cape Grim is at similar latitude to Wellington and also frequently receives air from the Southern Ocean (Levin et al., 2010). Samples are collected by a similar method to the Wellington record using NaOH absorption and are measured by gas counting to ~2 ‰ precision. Next we compare with mid-latitude high-altitude clean air sites in the Northern Hemisphere. The Vermunt, Austria (VER, 47.07°N, 9.57°E, 1800 m asl) record began in 1958, only a few years after the Wellington record began, and in the 1980s the site was moved to Jungfraujoch, Switzerland (JFJ, 46.55°N, 7.98°E, 3450 m asl); these measurements are made in the same manner and by the same laboratory as the Cape Grim record (Levin et al., 2013). We also consider the Niwot Ridge, USA $\Delta^{14}CO_2$ record (NWR, 40.05°N, 105.59°W, 3523 m asl), which began in 2003 (Turnbull et al., 2007; Lehman et al., 2013). Niwot Ridge is also a mid-latitude high-altitude site, but samples are collected as whole air in flasks and measured by AMS in a similar manner to that described for the Wellington flask samples. Thus, we are comparing two independent Southern Hemisphere records with two independent Northern Hemisphere records, with the two hemispheres tied together by the common measurement laboratory used for Cape Grim and Jungfraujoch. Results from all records are compared in figure 7.

The Wellington and Cape Grim records are generally consistent with one another, with the exception of the 1995-2005 period when the Wellington record is slightly higher, apparently due to bias in the Wellington record (discussed in section 3.5.3.). Differences between the sites are smaller than the measurement uncertainty for all other periods (table 2). This implies that the $\Delta^{14}CO_2$ signal is homogenous across Southern Hemisphere clean air sites within the same latitude band, at least since the 1980s when the two records overlap. Similarly, the high altitude, mid-latitude Northern Hemisphere sites are consistent with one another, although there are some differences in seasonal cycles in recent years (Turnbull et al., 2009).

The bomb spike is higher and earlier in the Northern Hemisphere records (figure 7), consistent with the production of most bomb ^{14}C in the Northern Hemisphere stratosphere (figure 5). We determine a new estimate for the interhemispheric exchange time from the difference in timing of the first maximum of the bomb peak in each hemisphere (July 1963 in the Northern Hemisphere, January 1965 in the Southern Hemisphere) as 1.4 years. This is consistent with other more detailed interhemispheric exchange time estimates that have been determined from long-term measurements of SF_6 of 1.3 to 1.4 years (Geller at el., 1997; Patra et al., 2011).

Atmos. Chem. Phys. Discuss., doi:10.5194/acp-2016-1110, 2016
Manuscript under review for journal Atmos. Chem. Phys.
Published: 20 December 2016

Atmospheric Chemistry and Physics Discussions

Northern Hemisphere $\Delta^{14}CO_2$ remains higher than Southern Hemisphere $\Delta^{14}CO_2$ by about 20 ‰ until 1972. Although most nuclear weapons testing ceased in 1963, a few smaller tests continued in the late 1960s, contributing to this continued interhemispheric offset (Enting, 1982). The interhemispheric gradient disappeared within about 1.5 years after atmospheric testing essentially stopped in 1970. Except periods of noisy data from Vermunt in the late 1970s and Wellington in 1995-2005, there are only small (<2 ‰) interhemispheric gradients from 1972 until 2002 (figure 7, table 2).

From 2002, an interhemispheric gradient of 5-7 ‰ develops, with the Southern Hemisphere sites higher than the Northern Hemisphere sites (table 2). We choose 1986 – 1990 and 2005 – 2013 as time periods to compare, to avoid the periods where the Wellington record is noisy (1995 – 2005) and where we substituted flask measurements from 1990 – 1993. In 1986 – 1990, there is less than 2 ‰ difference between Wellington and either Cape Grim or Jungfraujoch. There is also no difference between the Cape Grim and Jungfraujoch records during this time period. The Wellington and Cape Grim records still agree within 2 ‰ after 2005, but both Jungfraujoch and Niwot Ridge diverge from Wellington, by 4.8 ± 2.7 and 6.9 ± 2.5 ‰, respectively; they are not significantly different from one another. This new interhemispheric gradient is robust, being consistent amongst the sites measured by three different research groups each with their own methods. It is not an artifact of interlaboratory offsets, since Cape Grim and Jungfraujoch measurements are made by the same group using the same sampling and measurement methods, and the Wellington and Niwot Ridge measurements (measured by different techniques) agree well with the other sites at similar latitude (Cape Grim and Jungfraujoch respectively). This developing gradient is also apparent in 2005 – 2007 in a separate $\Delta^{14}CO_2$ sampling network (Graven et al., 2012), although that dataset extends only to 2007. Graven et al. (2012) demonstrated that increasing (mostly Northern Hemisphere) fossil fuel CO_2 emissions cannot explain this gradient, and instead, they postulated that ^{14}C uptake into the Southern Ocean reduced over time.

The development of the interhemispheric $\Delta^{14}CO_2$ gradient coincides with an apparent reorganization of Southern Ocean carbon exchange in the early 2000s (Landschützer et al., 2015). The net Southern Ocean carbon sink is determined by the balance between CO_2 uptake into surface waters, which are then subducted and sequester carbon, and release of carbon to the atmosphere from upwelling of very old, carbon-rich deep waters. CO_2 uptake into surface waters cannot change atmospheric $\Delta^{14}CO_2$, since the $\Delta^{14}C$ notation includes a mathematical correction for natural isotopic fractionation. In contrast, the ^{14}C disequilibrium between old (and therefore ^{14}C-poor), deep waters and the atmosphere means that release of CO_2 from the Southern Ocean to the atmosphere decreases atmospheric $\Delta^{14}CO_2$; the magnitude of that decrease depends on both the carbon flux and the ^{14}C disequilibrium. Thus, since the 1980s, atmospheric $\Delta^{14}C$ has been highly sensitive to Southern Ocean upwelling, the same mechanism that governs the ocean CO_2 sink (Graven et al., 2012). Model simulations suggest that changes in Southern Ocean ventilation may have played a key role in pre-industrial variations in the latitudinal gradient of atmospheric $^{14}CO_2$ (Rodgers et al., 2011).

Atmos. Chem. Phys. Discuss., doi:10.5194/acp-2016-1110, 2016
Manuscript under review for journal Atmos. Chem. Phys.
Published: 20 December 2016

Several studies using both data and modeling suggests that the climate-induced increase in westerly winds over the Southern Ocean increased upwelling of carbon-rich deep waters and thus reduced the Southern Ocean CO_2 sink efficiency (Le Quéré et al., 2007; Sitch et al., 2015). Yet, more recent evidence suggests a reinvigorated Southern Ocean carbon sink since about 2002 (Munro et al., 2016; Landschützer et al., 2015). These studies suggest that multiple factors contributed to the reinvigorated carbon sink, with different controls in the different Southern Ocean regions; these data support a decreasing upwelling of old, deep waters in recent years. Decreased upwelling would also cause a relative increase in Southern Hemisphere $\Delta^{14}CO_2$ and thus drive the observed interhemispheric $\Delta^{14}CO_2$ gradient, which appears at the same time as the apparent reinvigoration of the carbon sink in the early 2000s.

Although the changing Southern Ocean carbon sink is the most likely explanation, substantial underreporting of Northern Hemisphere fossil CO_2 emissions (e.g. Francey et al., 2013) or changes in the land carbon sink (Sitch et al., 2015; Wang et al., 2013) could also explain the new interhemispheric $\Delta^{14}CO_2$ gradient.

5. Conclusions

The 60 year-long Wellington $\Delta^{14}CO_2$ record has been revised and extended to 2014. Most revisions were minor, but we particularly note that the earlier reported 1990-1993 measurements have been entirely replaced with new measurements. A second period form 1995-2005 has poorer data quality than the rest of the record, and may also be biased high by a few permil. These data have been revised substantially, and new measurements have been added to this period, but we were unable to definitively identify or correct for bias, so the data have been retained, albeit with caution. We further validated the record by comparison with tree ring samples collected from the Baring Head sampling location and from nearby Eastbourne, Wellington; both tree ring records show excellent agreement with the original record, and indicate that there are no other periods where the original measurements are problematic.

The Wellington $\Delta^{14}CO_2$ time series records the history of atmospheric nuclear weapons testing and the subsequent decline of $\Delta^{14}CO_2$ as the bomb ^{14}C moved throughout the carbon cycle, and ^{14}C-free fossil fuel emissions further decreased $\Delta^{14}CO_2$. The timing of the first appearance of the bomb-^{14}C peak at Wellington is consistent with other recent estimates of interhemispheric exchange time at 1.4 years.

The seasonal cycle at Wellington evolves through the record, apparently dominated by the seasonality of cross-tropopause transport, which drives a changing seasonal cycle through time. In the early post-bomb period, the Southern Hemisphere troposphere was enriched in ^{14}C relative to the Southern Hemisphere stratosphere so that the seasonal minimum occurred at Wellington when cross-tropopause transport is at a maximum. The seasonal cycle reversed once the bomb perturbation reduced and continuing natural cosmogenic production meant that the Southern Hemisphere stratosphere was once again enriched in ^{14}C relative to the troposphere. In recent years, the seasonal cycle has amplitude of only 2 ‰, with a maximum in the austral spring. Cape Grim exhibits a similar seasonal cycle magnitude, but appears to be slightly influenced by a

Atmos. Chem. Phys. Discuss., doi:10.5194/acp-2016-1110, 2016
Manuscript under review for journal Atmos. Chem. Phys.
Published: 20 December 2016

terrestrial/anthropogenic signal during the austral winter that is not apparent at Wellington.

During the 1980s and 1990s, $\Delta^{14}CO_2$ was similar at mid-latitude clean air sites in both hemispheres, but since the early 2000s, the Northern Hemisphere $\Delta^{14}CO_2$ has dropped below the Southern Hemisphere by 5-7 ‰. This is most likely due to a change in Southern Ocean dynamics reducing upwelling of old, ^{14}C-poor deep waters, which is consistent with recent evidence for an increasing Southern Ocean carbon sink. This result implies that ongoing and expanded Southern Hemisphere $\Delta^{14}CO_2$ observations and modelling can provide a fundamental constraint on our understanding of Southern Ocean dynamics and exchange processes.

6. Acknowledgements

A 60 year-long record takes more than a handful of authors to produce. This work was possible only because of the amazing foresight and scientific understanding of Athol Rafter and Gordon Fergusson, who began this record in the 1950s. Their work was continued over the years by a number of people, including Hugh Melhuish, Martin Manning, Dave Lowe, Rodger Sparks, Charlie McGill, Max Burr and Graeme Lyon. This work was funded by the Government of New Zealand as GNS Science Global Change Through Time core funding and NIWA Greenhouse Gases, Emissions, and Carbon Cycle Science Programme core funding. The author(s) wish to acknowledge the contribution of New Zealand eScience Infrastructure (NeSI) to the results of this research. New Zealand's national compute and analytics services and team are supported by the NeSI and funded jointly by NeSI's collaborator institutions and through the Ministry of Business, Innovation and Employment (http://www.nesi.org.nz).

Atmos. Chem. Phys. Discuss., doi:10.5194/acp-2016-1110, 2016
Manuscript under review for journal Atmos. Chem. Phys.
Published: 20 December 2016

7. References

AECOM New Zealand Limited, 2016. Community greenhouse gas inventory for Wellington City and the Greater Wellington Region 2000-2015, Wellington.

Australian Government, 2016. State and territory greenhouse gas inventories 2014. Department of the Environment.

Baisden, W.T., Prior, C.A., Chambers, D., Canessa, S., Phillips, A., Bertrand, C., Zondervan, A., Turnbull, J.C., 2013. Radiocarbon sample preparation and data flow at Rafter: Accommodating enhanced throughput and precision. Nuclear Instruments and Methods B294, 194-198.

Boden, T.A., Marland, G., Andres, R.J., 2012. Global, Regional, and National Fossil-Fuel CO_2 Emissions. Carbon Dioxide Information Analysis Center, Oak Ridge National Laboratory, U.S. Department of Energy, Oak Ridge, Tenn., U.S.A.

Bozhinova, D., Combe, M., Palstra, S.W.L., Meijer, H.A.J., Krol, M.C., Peters, W., 2013. The importance of crop growth modeling to interpret the $^{14}CO_2$ signature of annual plants. Global Biogeochemical Cycles 27, 792-803.

Brailsford, G.W., Stephens, B.B., Gomez, A.J., Riedel, K., Mikaloff Fletcher, S.E., Nichol, S.E., Manning, M.R., 2012. Long-term continuous atmospheric CO_2 measurements at Baring Head, New Zealand. Atmospheric Measurement Techniques 5, 3109-3117.

Broecker, W.S., Peng, T.-H., Ostlund, H., Stuiver, M., 1985. The distribution of bomb radiocarbon in the ocean. Journal of Geophysical Research C4, 6953-6970.

Caldeira, K., Rau, G.H., Duffy, P.B., 1998. Predicted net efflux of radiocarbon from the ocean and increase in atmospheric radiocarbon content. Geophysical Research Letters 25, 3811-3814.

Currie, K.I., Brailsford, G., Nichol, S., Gomez, A., Sparks, R., Lassey, K.R., Riedel, K., 2011. Tropospheric $^{14}CO_2$ at Wellington, New Zealand: the world's longest record. Biogeochemistry 104, 5-22.

Davies, T., Cullen, M. J. P., Malcolm, A. J., Mawson, M. H., Staniforth, A., White, A. A., and Wood, N.: A new dynamical core for the Met Office's global and regional modelling of the atmosphere, Quarterly Journal of the Royal Meteorological Society, 131, 1759-1782, 2005.

Djuricin, S., Pataki, D.E., Xu, X., 2010. A comparison of tracer methods for quantifying CO_2 sources in an urban region. Journal of Geophysical Research 115.

Enting, I.G., 1982. Nuclear weapons data for use in carbon cycle modelling. CSIRO Division of Atmospheric Physics and Technology, Melbourne, Australia.

Ferretti, D.F., Lowe, D.C., Martin, R.H., Brailsford, G.W., 2000. A new gas chromatograph-isotope ratio mass spectrometry technique for high-precision, N_2O-free analysis of $\delta^{13}C$ and $\delta^{18}O$ in atmospheric CO_2 from small air samples. Journal of Geophysical Research Atmospheres 105, 6709-6718.

Francey, R.J., Trudinger, C.M., van der Schoot, M., Law, R.M., Krummel, P.B., Langenfelds, R.L., Steele, L.P., Allison, C.E., Stavert, A.R., Andres, R.J., Rödenbeck, C., 2013. Atmospheric verification of anthropogenic CO_2 emission trends. Nature Climate Change 3, 520-524.

Geller, L.S., Elkins, J.W., Lobert, J.M., Clarke, A.D., Hurst, D.F., Butler, J.H., Myers, R.C., 1997. Tropospheric SF_6: Observed latitudinal distribution and trends, derived

emissions and interhemispheric exchange time. Geophysical Research Letters 24, 675-678.

Graven, H.D., Gruber, N., 2011. Continental-scale enrichment of atmospheric $^{14}CO_2$ from the nuclear power industry: potential impact on the estimation of fossil fuel-derived CO_2. Atmospheric Chemistry and Physics 11, 12339-12349.

Graven, H.D., Guilderson, T.P., Keeling, R.F., 2012. Observations of radiocarbon in CO_2 at seven global sampling sites in the Scripps flask network: Analysis of spatial gradients and seasonal cycles. Journal of Geophysical Research 117.

Hogg, A.G., 2013. SHCAL13 Southern Hemisphere calibration, 0-50,000 years CAL BP. Radiocarbon.

Hua, Q., Barbetti, M., Jacobsen, G., Zoppi, U., Lawson, E., 2000. Bomb radiocarbon in annual tree rings from Thailand and Australia. Nuc. Inst. and Meth. in Physics Research B 172, 359-365.

Hua, Q., Barbetti, M., Rakowski, A.Z., 2013. Atmospheric radiocarbon for the period 1950-2010. Radiocarbon 55, 1-14.

Jones, A., Thomson, D., Hort, M., and Devenish, B.: The UK Met Office's next-generation atmospheric dispersion model, NAME III, Air Pollution Modeling and its Application XVII, 580-589, 2007.

Kanu, A., Comfort, L., Guilderson, T.P., Cameron-Smith, P.J., Bergmann, D.J., Atlas, E.L., Schauffler, S., Boering, K.A., 2015. Measurements and modelling of contemporary radiocarbon in the stratosphere. Geophysical Research Letters 43.

Keeling, C.D., Piper, S.C., Whorf, T.P., Keeling, R.F., 2011. Evolution of natural and anthropogenic fluxes of atmospheric CO2 from 1957 to 2003. Tellus B 63, 1-22.

Keeling, C.D., Whorf, T., 2005. Atmospheric CO_2 records from sites in the SIO air sampling network, Trends: A compendium of data of global change. Carbon Dioxide Information Analysis Center, Oak Ridge National Laboratory, Oak Ridge, Tenn., USA.

Key, R.M., 2004. A global ocean carbon climatology: Results from Global Data Analysis Project (GLODAP). Global Biogeochemical Cycles 18.

Kjellström, E., Feichter, J., Hoffman, G., 2000. Transport of SF_6 and $^{14}CO_2$ in the atmospheric general circulation model ECHAM4. Tellus 52B, 1-18.

Landschützer, P., Gruber, N., Haumann, F.A., Rödenbeck, C., Bakker, D.C.E., van Heuven, S., Hoppema, M., Metzl, N., Sweeney, C., Takahashi, T., Tilbrook, B., Wanninkhof, R., 2015. The reinvigoration of the Southern Ocean carbon sink. Science 349, 1221-1224.

Law, R.M., Steele, L.P., Krummel, P.B., Zahorowski, W., 2010. Synoptic variations in atmospheric CO_2 at Cape Grim: a model intercomparison. Tellus B 62, 810-820.

Le Quéré, C., Rödenbeck, C., Buitenhuis, E.T., Conway, T.J., Langenfelds, R., Gomez, A., Labuschagne, C., Ramonet, M., Nakazawa, T., Metzl, N., Gillett, N., Heimann, M., 2007. Saturation of the Southern Ocean CO_2 Sink Due to Recent Climate Change. Science 316, 1735-1738.

Lehman, S.J., Miller, J.B., Wolak, C., Southon, J.R., Tans, P.P., Montzka, S.A., Sweeney, C., Andrews, A.E., LaFranchi, B.W., Guilderson, T.P., Turnbull, J.C., 2013. Allocation of terrestrial carbon sources using $^{14}CO_2$: Methods, measurement, and modelling. Radiocarbon 55, 1484-1495.

742 Levin, I., Kromer, B., Hammer, S., 2013. Atmospheric $\Delta^{14}CO_2$ trend in Western
743 European background air from 2000 to 2012. Tellus B 65.
744 Levin, I., Kromer, B., Schmidt, M., Sartorius, H., 2003. A novel approach for
745 independent budgeting of fossil fuel CO_2 over Europe by $^{14}CO_2$ observations.
746 Geophysical Research Letters 30, 2194.
747 Levin, I., Kromer, B., Schoch-Fischer, H., Bruns, M., Munnich, M., Berdau, D., Vogel,
748 J.C., Munnich, K.O., 1985. 25 years of tropospheric ^{14}C observations in central
749 Europe. Radiocarbon 27, 1-19.
750 Levin, I., Naegler, T., Kromer, B., Diehl, M., Francey, R.J., Gomez-Pelaez, A.J., Steele,
751 L.P., Wagenbach, D., Weller, R., Worthy, D.E., 2010. Observations and modelling
752 of the global distribution and long-term trend of atmospheric $^{14}CO_2$. Tellus B 62,
753 26-46.
754 Lopez, M., Schmidt, M., Delmotte, M., Colomb, A., Gros, V., Janssen, C., Lehman, S.J.,
755 Mondelain, D., Perrussel, O., Ramonet, M., Xueref-Remy, I., Bousquet, P., 2013.
756 CO, NOx and $^{13}CO_2$ as tracers for fossil fuel CO_2: results from a pilot study in Paris
757 during winter 2010. Atmospheric Chemistry and Physics 13, 7343-7358.
758 Lowe, D.C., Judd, W., 1987. Graphite target preparation for radiocarbon dating by
759 accelerator mass spectrometry. Nuclear Instruments and Methods in Physics
760 Research B 28, 113-116.
761 Manning, M.R., Lowe, D.C., Melhuish, W.H., Sparks, R.J., Wallace, G., Brenninkmeijer,
762 C.A.M., McGill, R.C., 1990. The use of radiocarbon measurements in atmospheric
763 sciences. Radiocarbon 32, 37-58.
764 Meijer, H.A.J., Pertuisot, M.-H., van der Plicht, J., 2006. High accuracy ^{14}C
765 measurements for atmospheric CO_2 samples by AMS. Radiocarbon 48, 355-372.
766 Miller, J.B., Lehman, S.J., Montzka, S.A., Sweeney, C., Miller, B.R., Wolak, C.,
767 Dlugokencky, E.J., Southon, J.R., Turnbull, J.C., Tans, P.P., 2012. Linking
768 emissions of fossil fuel CO_2 and other anthropogenic trace gases using atmospheric
769 $^{14}CO_2$. Journal of Geophysical Research 117, D08302.
770 Munro, D.R., Lovenduski, N.S., Takahashi, T., Stephens, B.B., Newberger, T., Sweeney,
771 C., 2015. Recent evidence for a strengthening CO2sink in the Southern Ocean from
772 carbonate system measurements in the Drake Passage (2002-2015). Geophysical
773 Research Letters, n/a-n/a.
774 Naegler, T., Ciais, P., Rodgers, K., Levin, I., 2006. Excess radiocarbon constraints on air-
775 sea gas exchange and the uptake of CO_2 by the oceans. Geophysical Research
776 Letters 33.
777 Naegler, T., Levin, I., 2009. Observation-based global biospheric excess radiocarbon
778 inventory 1963–2005. Journal of Geophysical Research 114.
779 Norris, M.W., 2015. Reconstruction of historic fossil CO_2 emissions using radiocarbon
780 measurements from tree rings, School of Geography, Environment and Earth
781 Sciences. Victoria University of Wellington.
782 Nydal, R., Lövseth, K., 1983. Tracing bomb ^{14}C in the atmosphere 1962-1980. Journal of
783 Geophysical Research 88, 3621-3642.
784 Oeschger, H., Siegenthaler, U., Schotterer, U., Gugelmann, A., 1975. A box diffusion
785 model to study the carbon dioxide exchange in nature. Tellus XXVII, 168-192.

Atmos. Chem. Phys. Discuss., doi:10.5194/acp-2016-1110, 2016
Manuscript under review for journal Atmos. Chem. Phys.
Published: 20 December 2016

786 Olsen, M.A., Douglass, A.R., Schoeberl, M.R., 2003. A comparison of Northern and
787 Southern Hemisphere cross-tropopause ozone flux. Geophysical Research Letters
788 30.
789 Otago Daily Times, 1957. Polar ice caps may melt with industrialization, Otago Daily
790 Times, 23/1/1957 ed, Dunedin, New Zealand, p. 1.
791 Patra, P.K., Houweling, S., Krol, M., Bousquet, P., Belikov, D., Bergmann, D., Bian, H.,
792 Cameron-Smith, P., Chipperfield, M.P., Corbin, K., Fortems-Cheiney, A., Fraser,
793 A., Gloor, E., Hess, P., Ito, A., Kawa, S.R., Law, R.M., Loh, Z., Maksyutov, S.,
794 Meng, L., Palmer, P.I., Prinn, R.G., Rigby, M., Saito, R., Wilson, C., 2011.
795 TransCom model simulations of CH_4 and related species: linking transport, surface
796 flux and chemical loss with CH_4 variability in the troposphere and lower
797 stratosphere. Atmospheric Chemistry and Physics 11, 12813-12837.
798 Pickers, P.A., Manning, A.C., 2015. Investigating bias in the application of curve fitting
799 programs to atmospheric time series. Atmospheric Measurement Techniques 8,
800 1469-1489.
801 Rafter, T.A., 1955. ^{14}C variations in nature and the effect on radiocarbon dating. New
802 Zealand Journal of Science and Technology B37.
803 Rafter, T.A., Fergusson, G., 1959. Atmospheric radiocarbon as a tracer in geophysical
804 circulation problems, United Nations Peaceful Uses of Atomic Energy. Pergamon
805 Press, London.
806 Randerson, J.T., Enting, I.G., Schuur, E.A.G., Caldeira, K., Fung, I.Y., 2002. Seasonal
807 and latitudinal variability of troposphere $\Delta^{14}CO_2$: Post bomb contributions from
808 fossil fuels, oceans, the stratosphere, and the terrestrial biosphere. Global
809 Biogeochemical Cycles 16, 1112.
810 Reimer, P.J., Brown, T.A., Reimer, R.W., 2004. Discussion: Reporting and calibration of
811 post-bomb ^{14}C data. Radiocarbon 46, 1299-1304.
812 Rodgers, K.B., Mikaloff-Fletcher, S.E., Bianchi, D., Beaulieu, C., Galbraith, E.D.,
813 Gnanadesikan, A., Hogg, A.G., Iudicone, D., Lintner, B.R., Naegler, T., Reimer,
814 P.J., Sarmiento, J.L., Slater, R.D., 2011. Interhemispheric gradient of atmospheric
815 radiocarbon reveals natural variability of Southern Ocean winds. Climate of the
816 Past 7, 1123-1138.
817 Sitch, S., Friedlingstein, P., Gruber, N., Jones, S.D., Murray-Tortarolo, G., Ahlström, A.,
818 Doney, S.C., Graven, H., Heinze, C., Huntingford, C., Levis, S., Levy, P.E., Lomas,
819 M., Poulter, B., Viovy, N., Zaehle, S., Zeng, N., Arneth, A., Bonan, G., Bopp, L.,
820 Canadell, J.G., Chevallier, F., Ciais, P., Ellis, R., Gloor, M., Peylin, P., Piao, S.L.,
821 Le Quéré, C., Smith, B., Zhu, Z., Myneni, R., 2015. Recent trends and drivers of
822 regional sources and sinks of carbon dioxide. Biogeosciences 12, 653-679.
823 Steinkamp, K., Mikaloff Fletcher, S. E., Brailsford, G., Smale, D., Moore, S., Keller, E.
824 D., Baisden, W. T., Mukai, H., and Stephens, B. B., 2016. Atmospheric CO_2
825 observations and models suggest strong carbon uptake by forests in New Zealand,
826 Atmos. Chem. Phys. Discuss., doi:10.5194/acp-2016-254, in press, 2016.
827 Stephens, B.B., Brailsford, G.W., Gomez, A.J., Riedel, K., Mikaloff Fletcher, S.E.,
828 Nichol, S., Manning, M., 2013. Analysis of a 39-year continuous atmospheric CO_2
829 record from Baring Head, New Zealand. Biogeosciences 10, 2683-2697.
830 Stuiver, M., Polach, H.A., 1977. Discussion: Reporting of ^{14}C data. Radiocarbon 19, 355-
831 363.

832 Stuiver, M., Quay, P.D., 1981. Atmospheric 14C changes resulting from fossil fuel CO2
833 release and cosmic ray flux variability. Earth and Planetary Science Letters, 53,
834 349-362.
835 Suess, H.E., 1955. Radiocarbon concentration in modern wood. Science 122, 414-417.
836 Sweeney, C., Gloor, E., Jacobson, A.R., Key, R.M., McKinley, G., Sarmiento, J.L.,
837 Wanninkhof, R., 2007. Constraining global air-sea gas exchange for CO_2 with
838 recent bomb ^{14}C measurements. Global Biogeochemical Cycles 21.
839 Tans, P.P., De Jong, A.F., Mook, W.G., 1979. Natural atmospheric ^{14}C variation and the
840 Suess effect. Nature 280, 826-828.
841 Thoning, K.W., Tans, P.P., Komhyr, W.D., 1989. Atmospheric carbon dioxide at Mauna
842 Loa Observatory 2. Analysis of the NOAA GMCC data, 1974-1985. Journal of
843 Geophysical Research 94, 8549-8563.
844 Trumbore, S.E., 2000. Age of soil organic matter and soil respiration: Radiocarbon
845 constraints on belowground C dynamics. Ecological Applications 10, 399-411.
846 Turnbull, J.C., 2006. Development of a high precision $^{14}CO_2$ measurement capability and
847 application to carbon cycle studies, Geological Sciences. University of Colorado,
848 Boulder, p. 132.
849 Turnbull, J.C., Miller, J.B., Lehman, S.J., Hurst, D.F., Peters, W., Tans, P.P., Southon,
850 J.R., Montzka, S.A., Elkins, J.W., Mondeel, D.J., Romashkin, P.A., Elansky, N.F.,
851 Shkorokhod, A., 2009. Spatial distribution of $\Delta^{14}CO_2$ across Eurasia:
852 Measurements from the TROICA-8 expedition. Atmospheric Chemistry and
853 Physics 9, 175-187.
854 Turnbull, J.C., Sweeney, C., Karion, A., Newberger, T., Lehman, S.J., Tans, P.P., Davis,
855 K.J., Lauvaux, T., Miles, N.L., Richardson, S.J., Cambaliza, M.O., Shepson, P.B.,
856 Gurney, K., Patarasuk, R., Razlivanov, I., 2015. Toward quantification and source
857 sector identification of fossil fuel CO2 emissions from an urban area: Results from
858 the INFLUX experiment. Journal of Geophysical Research: Atmospheres.
859 Turnbull, J.C., Zondervan, A., Kaiser, J., Norris, M., Dahl, J., Baisden, W.T., Lehman,
860 S.J., 2015. High-precision atmospheric $^{14}CO_2$ measurement at the Rafter
861 Radiocarbon Laboratory. Radiocarbon 57, 377-388.
862 Wang, Y., Li, M., Shen, L., 2013. Accelerating carbon uptake in the Northern
863 Hemisphere: evidence from the interhemispheric difference of atmospheric CO_2
864 concentrations. Tellus B 65.
865 Ziehn, T., 2014. Greenhouse gas network design using backward Lagrangian particle
866 dispersion modelling – Part 1: Methodology and Australian test case. Atmospheric
867 Chemistry and Physics 14.
868 Zondervan, A., Hauser, T., Kaiser, J., Kitchen, R., Turnbull, J.C., West, J.G., 2015.
869 XCAMS: The compact 14C accelerator mass spectrometer extended for 10Be and
870 26Al at GNS Science, New Zealand. Nuclear Instruments and Methods B361, 25-
871 33.
872 Zondervan, A., Sparks, R.J., 1996. Development plans for the AMS facility at the
873 Institute of Geological and Nuclear Sciences, New Zealand. Radiocarbon 38, 133-
874 134.

Atmos. Chem. Phys. Discuss., doi:10.5194/acp-2016-1110, 2016
Manuscript under review for journal Atmos. Chem. Phys.
Published: 20 December 2016

Atmospheric Chemistry and Physics Discussions

8. Tables

Date Range	NZ/NZA	Site	collection method	Measurement method
1954-1986	0-7500	MAK	tray	GC
1987-1994	7500-8400	BHD	tray	GC
1995-2004	8400-30000	BHD	bottle	ENTandem ^{13}C ^{14}C
2005-2009	30000-34000	BHD	bottle	ENTandem ^{12}C ^{13}C ^{14}C
2010-2011	34000-50000	BHD	bottle	XCAMS
2012-present	50000-	BHD	bottle	XCAMS/RG20

Table 1. Wellington $^{14}CO_2$ measurement methods through time.

Site difference	**Time period**	**$\Delta^{14}CO_2$ difference**
WLG-CGO	1986-1990	1.8 ± 2.5
WLG-CGO	2005-2013	1.3 ± 3.4
WLG-JFJ	1986-1990	0.8 ± 3.9
WLG-JFJ	2005-2013	4.8 ± 2.7
WLG-NWR	2005-2013	6.9 ± 2.5

Table 2. $\Delta^{14}CO_2$ gradients between sites, determined as the mean of the monthly differences for each time period. Errors are the standard deviation of the monthly differences.

Atmos. Chem. Phys. Discuss., doi:10.5194/acp-2016-1110, 2016
Manuscript under review for journal Atmos. Chem. Phys.
Published: 20 December 2016

Atmospheric Chemistry and Physics Discussions

9. Figures

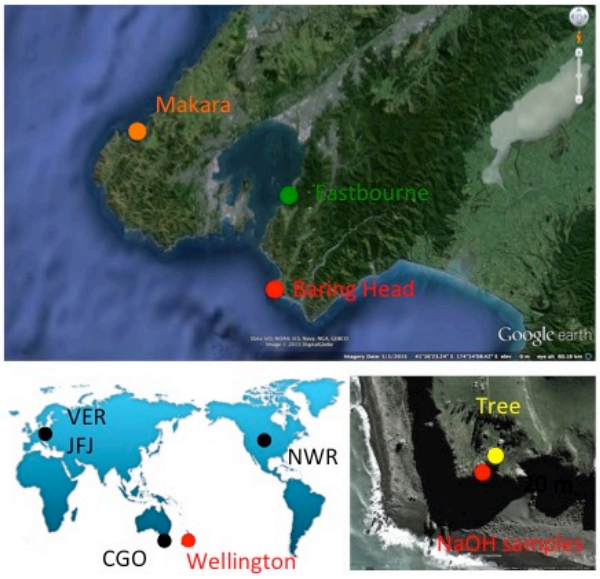

Figure 1. Sampling locations. Top: Makara (1954-1986) and Baring Head (1987 – present) air sampling sites and the location of the Eastbourne tree samples. Bottom left: world location showing Wellington and other sampling sites discussed in the text. Bottom right: close up of the Baring Head site showing the relative positions of the air (NaOH) and tree sampling locations.

Atmos. Chem. Phys. Discuss., doi:10.5194/acp-2016-1110, 2016
Manuscript under review for journal Atmos. Chem. Phys.
Published: 20 December 2016

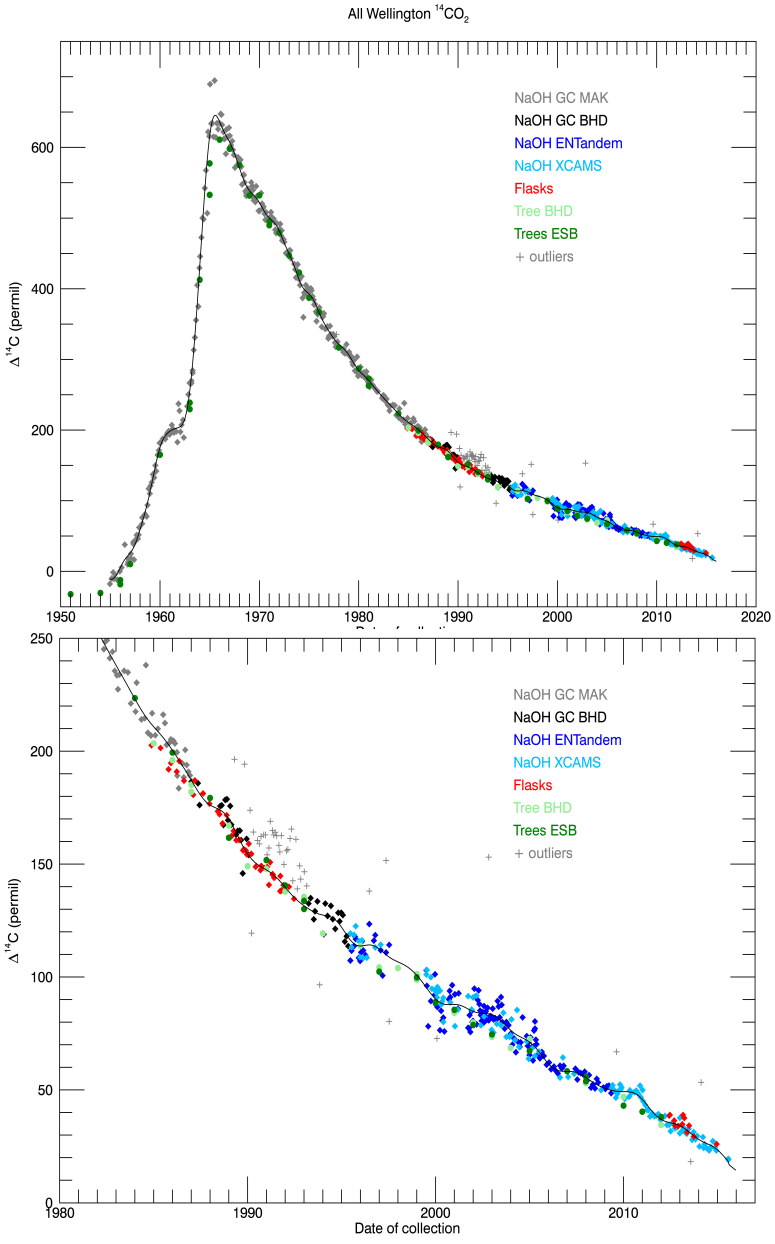

Figure 2. Wellington $^{14}CO_2$ record showing all collection and measurement methods. Tree rings (green) and outliers (grey pluses) are excluded from the reported final dataset. Black line is the smooth curve fit to the final dataset.

Atmos. Chem. Phys. Discuss., doi:10.5194/acp-2016-1110, 2016
Manuscript under review for journal Atmos. Chem. Phys.
Published: 20 December 2016

Atmospheric Chemistry and Physics Discussions

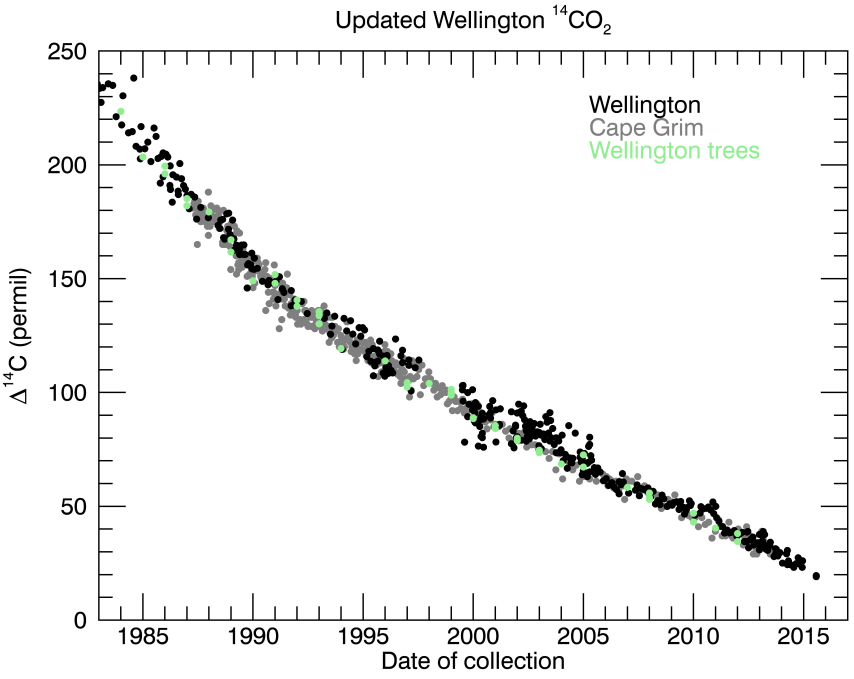

Figure 3. Comparison of the final Wellington and Cape Grim (Levin et al., 2010) $\Delta^{14}CO_2$ records. Wellington tree ring measurements are also shown.

Atmos. Chem. Phys. Discuss., doi:10.5194/acp-2016-1110, 2016
Manuscript under review for journal Atmos. Chem. Phys.
Published: 20 December 2016

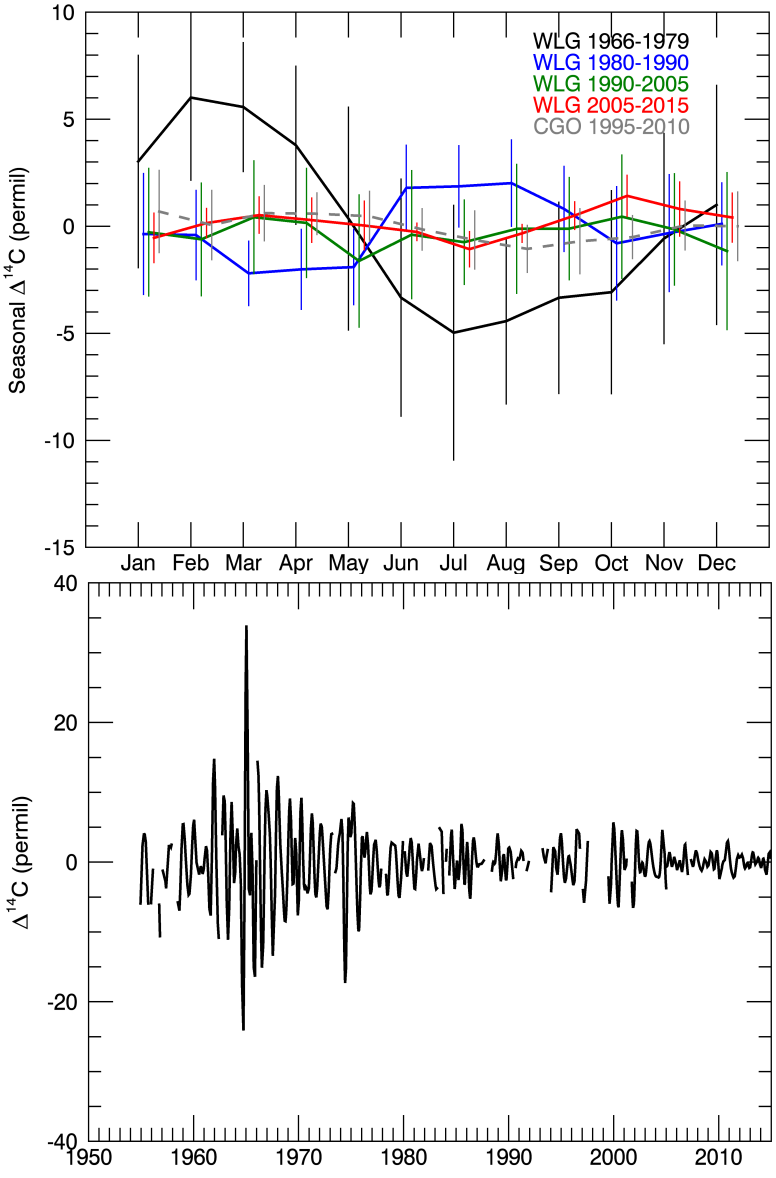

Figure 4. Detrended seasonal cycle in the Wellington $\Delta^{14}CO_2$ record. Top: WLG monthly detrended seasonal cycle averaged over four time periods as described in the text and the CGO (Levin et al., 2010) detrended seasonal cycle. Error bars are the standard deviation of all years averaged. Points for each time period are slightly offset for clarity. Bottom: full seasonal cycle record determined separately for each time period shown in the top panel plus 1954-1965.

Atmos. Chem. Phys. Discuss., doi:10.5194/acp-2016-1110, 2016
Manuscript under review for journal Atmos. Chem. Phys.
Published: 20 December 2016

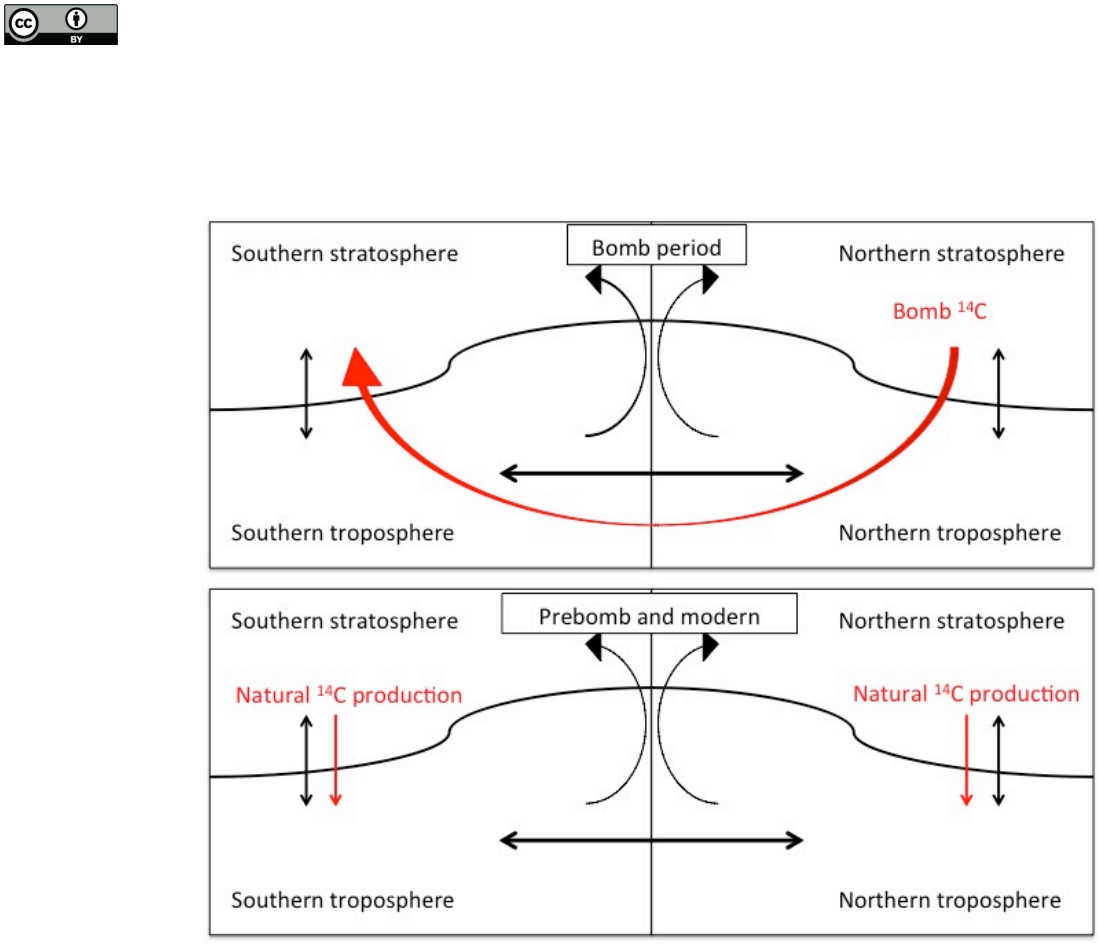

Figure 5. Schematic of stratosphere – troposphere circulation. Black lines show directions of mixing, and the red lines show the movement of ^{14}C. Top panel shows movement during the bomb period when bomb ^{14}C produced in the Northern stratosphere dominated over natural ^{14}C production and atmospheric transport quickly enriched the Southern troposphere relative to the Southern stratosphere. The bottom panel shows the pre- and post-bomb periods when natural ^{14}C production in both Northern and Southern stratospheres results in the Southern stratosphere being enriched relative to the underlying troposphere.

Atmos. Chem. Phys. Discuss., doi:10.5194/acp-2016-1110, 2016
Manuscript under review for journal Atmos. Chem. Phys.
Published: 20 December 2016

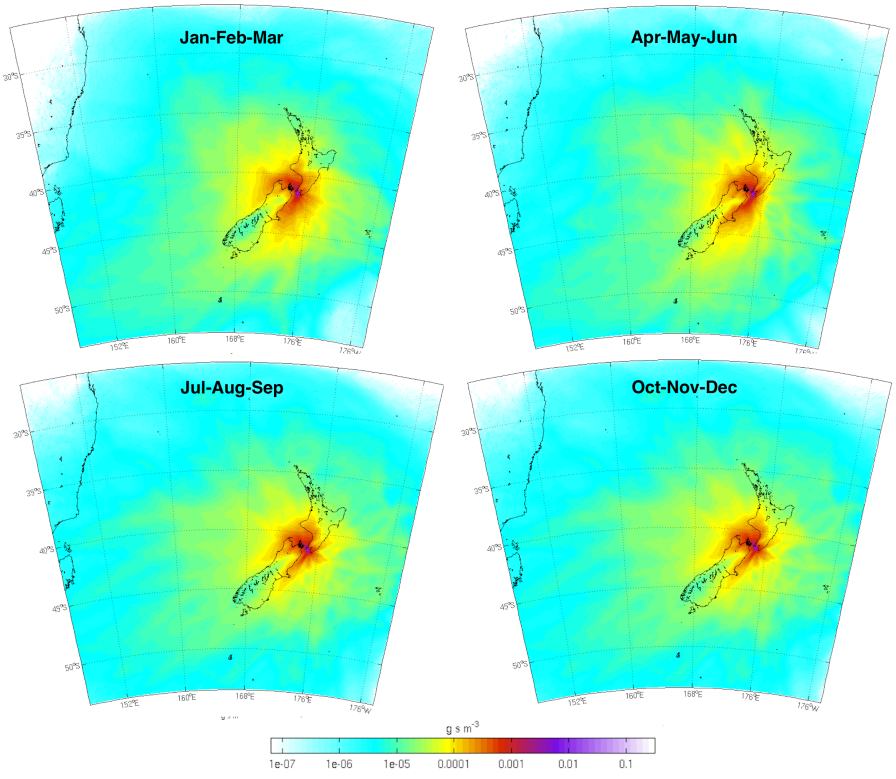

Figure 6. Mean footprints for the BHD site for each three-month period, averaged over the years 2011 – 2013. Footprints were determined using the NAME III atmospheric dispersion model forced with meteorology from the NZLAM weather prediction model.

Atmos. Chem. Phys. Discuss., doi:10.5194/acp-2016-1110, 2016
Manuscript under review for journal Atmos. Chem. Phys.
Published: 20 December 2016

Atmospheric Chemistry and Physics Discussions

928

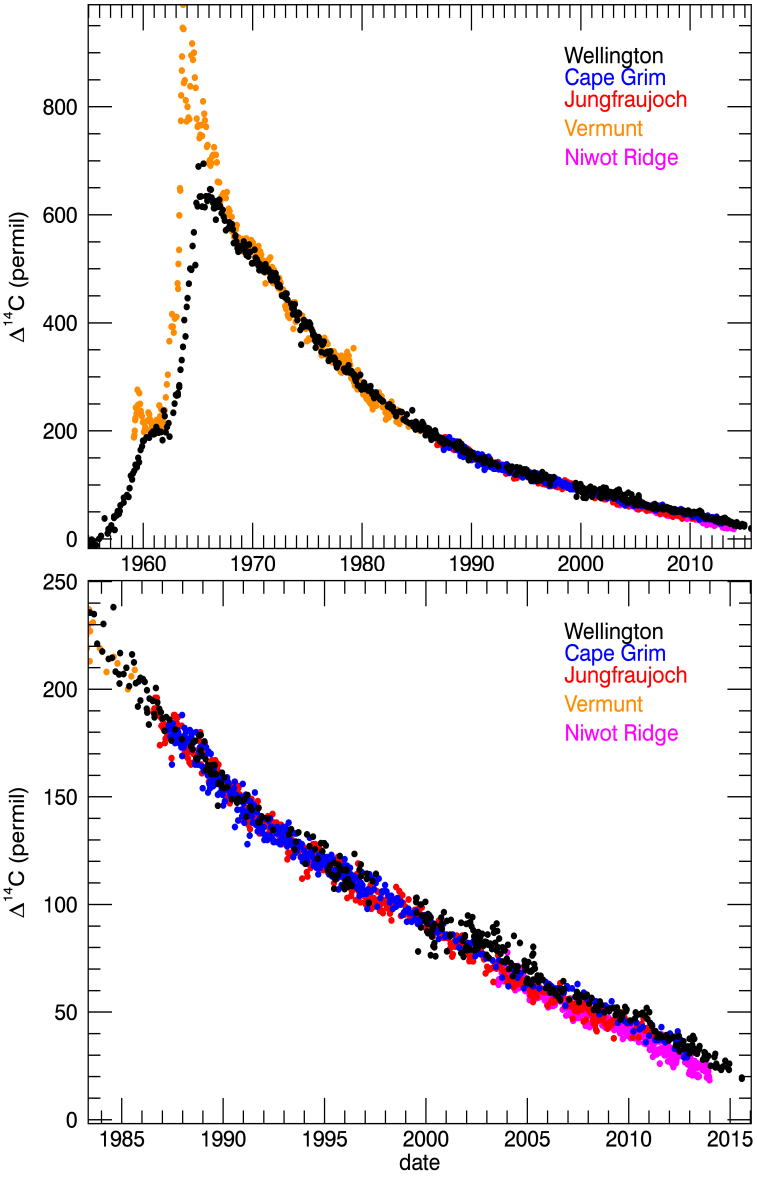

929
930
931 Figure 7. Comparison of Wellington and other atmospheric $\Delta^{14}CO_2$ records (Levin et al.,
932 2010; Turnbull et al., 2007; Lehman et al., 2013).